

Resonance approximation and charge loading and unloading in adiabatic quantum pumping

Vyacheslavs Kashcheyevs, Amnon Aharony, and Ora Entin-Wohlman

School of Physics and Astronomy, Raymond and Beverly Sackler faculty of Exact Sciences, Tel Aviv University, Tel Aviv 69978, Israel

(Received 19 August 2003; revised manuscript received 17 December 2003; published 6 May 2004)

Quantum pumping through mesoscopic quantum dots is known to be enhanced by resonant transmission. The pumped charge is close to an integer number of electrons when the pumping contour surrounds a resonance, but the transmission remains small on the contour. For noninteracting electrons, we give a quantitative account of the detailed exchange of electrons between the dot and the leads (to the electron reservoirs) during a pumping cycle. Near isolated distinct resonances, we use approximate Breit-Wigner expressions for the dot's Green function to discuss the loading/unloading picture of the pumping: the fractional charge exchanged between the dot and each lead through a single resonance point is related to the relative couplings of the dot and the leads at this resonance. If each resonance point along the pumping contour is dominated by the coupling to a single lead (which also implies a very small transmission), then the crossing of each such resonance results in a single electron exchange between the dot and that lead, ending up with a net quantized charge. When the resonance approximation is valid, the fractional charges can also be extracted from the peaks of the transmissions between the various leads.

DOI: 10.1103/PhysRevB.69.195301

PACS number(s): 73.23.-b, 73.63.Rt, 72.10.-d, 73.40.Ei

I. INTRODUCTION

There has been much recent experimental¹⁻³ and theoretical⁴⁻¹⁷ interest in adiabatic quantum pumping through mesoscopic electronic devices, such as quantum channels or quantum dots (QD's). Typically, the QD is connected via leads to several electron reservoirs, and is subject to a slowly varying oscillating potential, with period $T = 2\pi/\omega$. Under appropriate conditions, the device yields a nonzero dc time-averaged current between pairs of terminals, even when the terminals have the same chemical potential. Under ideal conditions, the charge Q transferred between the terminals during a period T may be "quantized," i.e., very close to an integer times the electron charge e . Several recent theoretical studies have considered enhancement of the adiabatic pumping current due to resonant transmission¹⁸ through the QD, both for noninteracting^{9,11,16,19,20} and interacting electrons.²¹ Connections between pumped charge quantization and resonant transmission have been reported in different contexts.^{11,16,19,20,22,23}

Usually, the oscillating potential is characterized by several time-dependent parameters, $\{X_i(t)\}$. As time evolves during one period T , these parameters follow a closed contour in the parameter space. A schematic example is shown in Fig. 1 for two such parameters. In parallel to discussing pumping, one can also consider the conductance between pairs of terminals generated by an appropriate bias. This conductance, which depends on the parameters $\{X_{ij}\}$, may have resonance peaks in the same parameter space. In this context, one freezes the time dependence, and considers the conductance at some instantaneous values of the $\{X_{ij}\}$'s. It has been argued¹¹ that the pumped charge Q will be close to being quantized if the pumping contour surrounds such a peak (e.g., at the point M in Fig. 1), while staying at points with a low conductance.

In the present paper we present an approximate theory for adiabatic pumping of coherent noninteracting spinless electrons, which is valid for discrete and distinct resonances, and

use this approximation to obtain physical insight into the reasons for this quantization. Given a conductance peak (e.g., at the point M in Fig. 1), one can usually also identify a "resonance line," along which the conductance decreases from its peak more slowly than along other directions.^{11,16} Such a line is illustrated by the dashed line in Fig. 1. In the example shown in this figure, the resonance line is crossed by the pumping contour twice, at points B and D . Measuring the instantaneous biased conductance between the two relevant terminals for each time t during the oscillation period, one expects two local peaks at these two resonance points. Under appropriate conditions, which include the limit of weak QD-terminal coupling, most of the pumped current arises when the parameters are close to these resonance points: for example, one can identify a "loading" of the QD by some charge $\Delta Q_\alpha^{\text{res}}$, coming from terminal α , at the point B , and an "unloading" of the QD, by $\Delta Q_{\alpha'}^{\text{res}}$, into terminal α' , at the point D . The resulting total pumped charge per period approaches a robust, detail-independent value Q^R , which is determined *only* by the ratios of the coupling strengths between the QD and the different reservoirs at the

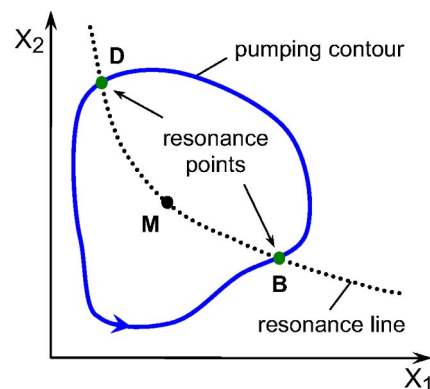


FIG. 1. (Color online) Schematic picture of a two-dimensional pumping contour, crossing the resonance line at two resonance points (B and D). The transmission is maximal at the point M .

resonance points. We also show that Q^R can be related quantitatively to the measured values of the peak conductances. Q^R is (almost) quantized (in units of e) when there is one dominant coupling for each resonance.

Our results can be summarized in a very simple and physically transparent way, by considering the occupation numbers of the quasibound state on the QD, corresponding to each transmission resonance. Each time the energy of such a state crosses the chemical potential μ (which is the same in all reservoirs), the QD gains or loses one electron, so that the total pumped charge flowing into it (per period) is quantized. However, the distribution of the pumped charge between different reservoirs is proportional to the corresponding coupling strengths (tunneling rates). Therefore the pumping current between any two leads can be obtained by summing up individual resonance contributions, with appropriate signs.

A similar “shuttling mechanism” for pumping has been used widely to interpret experiments^{2,3} in the Coulomb blockade regime, when the energetics on the QD is dominated by the electron-electron interactions.²⁴ In that approach, electrons are transferred from a lead to the dot and then from the dot to another lead, whenever such transfers are favored energetically. In contrast, Refs. 11,15,16,25 and 26 presented explicit quantum-mechanical calculations for pumping of noninteracting electrons, calculated the total charge pumped during a full cycle, and emphasized the role played by quantum interference in such processes. In some sense, the present paper bridges between these points of view: in the limit of weak coupling between the QD and the leads, we do end up with a loading/unloading picture, even for noninteracting electrons.⁴⁵ However, the details of the charge exchanges during a pumping cycle are found to be more complicated than in the “shuttling” picture: at a given resonance point, charge can usually be shared by several leads. Apart from this, the conditions for the applicability of our loading/unloading picture are similar to those of a single electron transistor,² in the sense that the role of quantum interference is restricted to the definition of independent single-particle resonances. In view of this, there is room to conjecture that some of our results may also apply in the presence of electron interactions.

The paper is organized as follows. In Sec. II we review the physical assumptions of the model and the formulas used for the calculation of the adiabatic current. We then use these formulas to derive the current for a single resonant state, by approximating the Green function on the QD by a Breit-Wigner-type formula. In Sec. III we obtain our main result—the adiabatically pumped charge for a sequence of well-defined distinct resonances—and discuss possible applications and experimental verification. To demonstrate this general picture, Sec. IV presents the analysis of the pumped charge for a simple model¹⁵ of a “turnstile” pumping device. A short summary concludes the paper in Sec. V.

II. ADIABATIC CURRENT

We consider a spatially confined nanostructure (the QD) connected by ideal leads to the electronic reservoirs with a common chemical potential μ and temperature T . The total

Hamiltonian for noninteracting spinless electrons is

$$\mathcal{H} = \mathcal{H}^d + \sum_{\alpha} (\mathcal{H}_{\alpha}^l + L_{\alpha} + L_{\alpha}^{\dagger}), \quad (1)$$

$$\mathcal{H}^d = \sum_{mn} h_{mn}(t) d_m^{\dagger} d_n \quad (\text{dot}), \quad (2)$$

$$\mathcal{H}_{\alpha}^l = \sum_k E_{\alpha k} c_{\alpha k}^{\dagger} c_{\alpha k} \quad (\text{leads}), \quad (3)$$

$$L_{\alpha} = \lambda_{\alpha}(t) \sum_{k,n} J_{\alpha kn} c_{\alpha k}^{\dagger} d_n \quad (\text{hopping}). \quad (4)$$

Here \mathcal{H}^d is the Hamiltonian of an N -state isolated QD ($n, m = 1, \dots, N$), the index $\alpha = 1, \dots, L$ enumerates the one-dimensional leads connected to the QD, $c_{\alpha k}^{\dagger}$ creates a standing wave $|w_{k\alpha}\rangle$ with wave number k and energy $E_{\alpha k}$ in the channel α , the operator L_{α} describes hopping from the QD into the channel α , and the λ_{α} 's are real dimensionless coefficients. For pumping we allow variation of $\mathcal{H}(t)$ via the time-dependent parameters h_{mn} and λ_{α} .

The instantaneous adiabatic current in the channel α , directed from a remote reservoir towards the QD, has been expressed in Ref. 15 as

$$I_{\alpha}(t) = \frac{e}{2\pi} \int dE f'(E) \mathcal{I}_{\alpha}, \quad \mathcal{I}_{\alpha} = \frac{1}{\hbar} \langle \chi_{k\alpha} | \dot{\mathcal{H}} | \chi_{k\alpha} \rangle, \quad (5)$$

where $f(E) = 1/[1 + e^{(E-\mu)/k_B T}]$ is the Fermi-Dirac distribution and $|\chi_{k\alpha}\rangle$ is the instantaneous scattering state normalized to a unit flux, $\langle \chi_{k\alpha} | \chi_{k'\alpha} \rangle = (2\pi/v_{k\alpha}) \delta(k-k')$, with $v_{k\alpha} = \partial E_{k\alpha} / \partial(\hbar k)$ being the velocity in the channel α .

In Appendix we use standard scattering theory formulas to rewrite this equation in the form

$$\mathcal{I}_{\alpha}(E, t) = \text{Tr}_d [G_d^{\dagger} (\dot{\mathcal{H}}^d + \dot{\hat{\Sigma}}) G_d \hat{\Gamma}_{\alpha} + (G_d + G_d^{\dagger}) \hat{\Gamma}_{\alpha} / 2]. \quad (6)$$

Here, the operators

$$G_d = (E + i0 - \mathcal{H}^d - \hat{\Sigma})^{-1}, \quad (7)$$

$$\hat{\Sigma} = \hat{\mathcal{E}} - i\hat{\Gamma}/2, \quad (8)$$

$$\hat{\Gamma} = \sum_{\alpha} \hat{\Gamma}_{\alpha}, \quad \hat{\Gamma}_{\alpha} = iL_{\alpha}^{\dagger} (G_{\alpha}^l - G_{\alpha}^{l\dagger}) L_{\alpha}, \quad (9)$$

$$\hat{\mathcal{E}} = \sum_{\alpha} \hat{\mathcal{E}}_{\alpha}, \quad 2\hat{\mathcal{E}}_{\alpha} = L_{\alpha}^{\dagger} (G_{\alpha}^l + G_{\alpha}^{l\dagger}) L_{\alpha} \quad (10)$$

act only on the subspace of the QD. Also, G_{α}^l denotes the retarded Green function of an isolated channel, $G_{\alpha}^l = (E + i0 - \mathcal{H}_{\alpha}^l)^{-1}$. We have separated the self-energy operator $\hat{\Sigma}$ into a sum of resonance width and shift operators,²⁷ $\hat{\Gamma}_{\alpha}$ and $\hat{\mathcal{E}}_{\alpha}$, which are Hermitian.

Equation (6) is a generalized version of the pumping current formula derived in Ref. 25 for a particular case of single-mode tight-binding (TB) leads and time-independent couplings.⁴⁶

The adiabatic current (6) can be calculated exactly, provided that one is able to compute the Green function (7) on the QD. We are interested in the regime when the transport is dominated by a single nondegenerate orbital state, and instead of Eq. (2) we consider

$$\mathcal{H}_{\text{res}}^d = \epsilon(t)|\psi\rangle\langle\psi| \equiv \epsilon(t)d^\dagger d. \quad (11)$$

The energy distance to the next resonant state Δ will be assumed to be much larger than all other energies. The Green function corresponding to $\mathcal{H}_{\text{res}}^d$ now assumes the Breit-Wigner-like form²⁸

$$G_d = \frac{|\psi\rangle\langle\psi|}{E - \epsilon - \langle\psi|\Sigma|\psi\rangle}. \quad (12)$$

The approximation of a single noninteracting energy level, Eq. (12), is valid for resonant tunneling structures with negligible charging energy, and corresponds to the Breit-Wigner treatment of mesoscopic electrical transport initiated in Refs. 29 and 30. For example, our results are directly applicable to the much studied double barrier pumping^{9,11,14,31,32} in the resonant tunneling regime.^{9,11} We also list several experimental situations when the charging energy is not small, but our noninteracting spinless model can still have some relevance. First, it applies when spin degeneracy is removed either by a constant in-plane magnetic field or by feeding the device with fully polarized electrons from half metallic ferromagnetic leads, e.g., CrO₂ (Ref. 33). In this case the energy scale Δ is set by the level spacing of the effective device Hamiltonian \mathcal{H}^d . Second, the Breit-Wigner approximation (12) is relevant for the Coulomb blockade peaks of a strongly pinched quantum dot well above the Kondo temperature.^{34,35} Specifically, within the Hartree approximation, a large on-site Coulomb repulsion energy U forbids double occupancy of otherwise spin-degenerate energy levels and sets the interresonance distance $\Delta = U$. Explicit derivation of the Breit-Wigner resonances for a weakly coupled interacting system can be found in Ref. 36.

Substitution of Eq. (12) into Eq. (6) gives

$$\mathcal{I}_\alpha = \frac{\Gamma_\alpha \dot{E}_0 - \dot{\Gamma}_\alpha (E_0 - E)}{(E - E_0)^2 + (\Gamma/2)^2}, \quad (13)$$

where $E_0(E, t) = \epsilon + \langle\psi|\hat{\mathcal{E}}|\psi\rangle$ and $\Gamma_\alpha(E, t) = \langle\psi|\hat{\Gamma}_\alpha|\psi\rangle$. Since the partial “width” Γ_α is of order $\lambda_\alpha^2 |J_{\alpha k}|^2$, it represents a measure for the coupling of the QD with the channel α . The exact adiabatic current for a single level given by Eq. (13) will be the starting point for our analysis of the pumped charge in Sec. III. Breit-Wigner-type expressions for the current pumped by a single orbital level have been derived previously in the weak pumping limit,²¹ and in the presence of interactions and Zeeman splitting.²² However, they were not used to discuss the details of the pumped charge quantization.

In the remainder of this section we discuss the physical interpretation of Eq. (13). The total current $I = \sum_\alpha I_\alpha$ represents changes in the total charge accumulated both on the dot and in the leads. For small dot-lead couplings, one would expect that the charge on the QD itself is a well-defined quantity and a simple picture of single electrons tunneling between the leads and the QD should apply. In order to clarify the relation between our quantum calculation and this “classical shuttling picture,” we comment on the localization of the charge.

Equation (13) implies that the total current in our model is a full time derivative, $I = dQ^F(E_0, \Gamma)/dt$ of some time-dependent charge $Q^F(t)$, where

$$Q^F(t) = -e \int dE f'(E) \left\{ \frac{1}{2} + \frac{1}{\pi} \arctan \frac{2(E - E_0)}{\Gamma} \right\}. \quad (14)$$

(We have chosen the integration constant such that Q^F/e is bounded between 0 and 1.) The charge Q^F represents the integrated Breit-Wigner density of states and can be interpreted^{37,38} as the additional charge induced in the system by an extra electronic state $|\psi\rangle$.

This delocalized charge Q^F is to be compared with the local equilibrium occupation inside the QD, which is given by $Q^{\text{occ}}/e = \text{Tr}[\rho|\psi\rangle\langle\psi|]$, where $\rho = h^{-1} \int dE f(E) \Sigma_\alpha |\chi_{k\alpha}\rangle\langle\chi_{k\alpha}|$ is the equilibrium density matrix corresponding to $\mathcal{H}(t)$.⁴⁷ Using Eqs. (A1), (A6), and (12) one can show that

$$Q^{\text{occ}} = \frac{e}{2\pi} \int dE f(E) \frac{\Gamma}{(E_0 - E)^2 + (\Gamma/2)^2}. \quad (15)$$

If E_0 and Γ were independent of E , then integration by parts would yield the equality $Q^{\text{occ}} = Q^F$. In general, E_0 and Γ do depend on E , and hence $Q^{\text{occ}} \neq Q^F$.

III. RESONANCE APPROXIMATION

The Breit-Wigner form (13) of the pumping current demonstrates a well-established fact^{9,11,16} that pumping is greatly enhanced near a resonance. The resonance condition is $|E_0 - \mu| \lesssim D$, where $D = \max(\Gamma, kT)$ is the energetic width of the resonance. One option, considered in Ref. 21, is to design the pumping contour in such a way that the system stays entirely at resonant transmission. In this case, the Breit-Wigner approximation does not lead to any pumped charge quantization.²¹ Here we focus on a more generic case, when the resonance condition is satisfied only during a small fraction of the pumping cycle, as the system goes through a resonance point. As shown in Refs. 11,16,19 and 20, this situation allows for pumped charge quantization. Specifically, we assume that the system remains near a resonance point only during a small fraction of the pumping cycle. This requires relatively narrow resonances, i.e., small widths D and therefore also small Γ .

Consider a resonance time t_R on the pumping contour, identified by the resonance condition $E_0(\mu, t_R) = \mu$. This identifies a “resonance point” on the contour. Assume also that the system “crosses” this resonance point completely

between times t_1 and t_2 , such that (1) Γ_α , E_0 are energy independent around the Fermi surface (for $|E - \mu| \leq kT$); (2) at the “boundary” times, the system is far from the resonance, $D \ll |E_0(\mu, t_{1,2}) - \mu| \ll \Delta$; (3) while at resonance, the couplings change negligibly, $|\dot{\Gamma}_\alpha| \ll |\dot{E}_0|$.

Under these conditions, we can integrate Eq. (13) and get the charge transferred from the reservoir α in a simple form:

$$\Delta Q_\alpha^{\text{res}} = \int_{t_1}^{t_2} dt I_\alpha = -e \frac{\Gamma_\alpha}{\Gamma} \text{sgn} \dot{E}_0 \quad (\text{at } E_0 = \mu). \quad (16)$$

For this particular resonance point, other parts of the pumping contour contribute negligibly to this charge. Equation (16) is our main result for the pumped charge due to a well-defined resonance point. We will refer to this result as “the resonance approximation.” In this approximation, each reservoir contributes on average a fraction of the electronic charge, which is proportional to the corresponding fractional decay width or coupling Γ_α/Γ . The total change in the charge accumulated in the system due to this particular resonance is thus

$$\Delta Q^{\text{res}} \equiv \sum_\alpha \Delta Q_\alpha^{\text{res}} = \pm e. \quad (17)$$

This result can be easily generalized for several independent resonance points. If the pumping contour can be separated into several parts, each containing a single well-defined resonance point, and if the pumping currents on the rest of the contour remain negligible, then the total charge Q_α^{R} , pumped through the channel α , is given by a sum over the resonances: $Q_\alpha^{\text{R}} = \sum_{\text{res}} \Delta Q_\alpha^{\text{res}}$. For a periodic $\mathcal{H}(t)$, the pumping contour is closed, and charge conservation $\sum_\alpha Q_\alpha^{\text{R}} = 0$ is ensured by Eq. (17) and the fact that the number of loading ($\dot{E}_0 < 0$) and unloading ($\dot{E}_0 > 0$) resonance points is the same.

A. Pumped charge quantization

Equation (17) can be interpreted as the loading/unloading of exactly one electron into/out of the QD, depending on the sign of \dot{E}_0 at the Fermi level. Furthermore, Eq. (16) implies that ΔQ_{res} is dominated by the current from a single channel α , provided that $\Gamma_\alpha \gg \Gamma_{\alpha'}$ for $\alpha \neq \alpha'$. If the same applies to all the resonances, then we end up with a “classical” picture, in which the pumping cycle contains a sequence of individual discrete events, of exchanging electrons one by one between a reservoir and the QD. After a full cycle, the charge on the QD will remain unchanged, and an integer number of electrons will have crossed the QD between any pair of reservoirs. This gives a detailed explanation of the pumped charge quantization within this approximation.

Using the same conditions as used to derive Eq. (16), one can show that both $\Delta Q^{\text{F}} \equiv Q^{\text{F}}(t_2) - Q^{\text{F}}(t_1)$ and ΔQ^{occ} are equal to ΔQ^{res} . This means that every time the system crosses a resonance point, the charge associated with the resonant state changes by $\sim \pm e$. Therefore we stress that if one is interested in the total charge pumped by a single resonance [and not, for example, in the line shape of the current,

Eq. (13)], then the simple picture of loading/unloading of a single electron, as reflected in Eq. (16), is applicable—regardless of the ratio Γ/kT .

We also note that for such an ideal quantization ($Q_{\alpha \rightarrow e}^{\text{R}} \times \text{integer}$), that is independent of the contour details, one would need to consider the limit $\Gamma_\alpha \approx \Gamma \rightarrow 0$ for each resonance; the resonance approximation becomes exact, with results which are independent of the details of the contour, when $\Gamma \rightarrow 0$, and the charge goes only via channel α when $\Gamma_\alpha/\Gamma \rightarrow 1$. As explained in the following section, this implies a vanishing transmission throughout the whole pumping cycle, in accordance with the conclusions of Refs. 11 and 39.

B. Relation to conductance

The criteria for the validity of the resonance approximation, listed in the preceding section, can be *quantitatively* checked in experiments (or in numerical calculations) by monitoring the conductance between different leads as a function of parameters along the pumping contour.^{11,16} A definitive signature of the relevant transport regime (for having a significant nonzero pumped charge) would be the presence of an even number of well-separated peaks in the conductance time trace: each resonance (M in Fig. 1) is associated with two peaks in the instantaneous transmission, encountered at the two resonance points (B and D) where the pumping contour crosses the resonance line on each side of the resonance, as schematically shown in Fig. 1. Note that this measurement is independent of time: one simply measures the conductance at different points on the pumping contour.

The contribution of each particular conductance peak to the pumped charge can be calculated along the following lines. Application of the general expression of the transmission probability²⁷ from channel α' to channel α , $\mathcal{T}_{\alpha\alpha'} = -\int dE f'(E) \text{Tr}[G_d^\dagger \hat{\Gamma}_\alpha G_d \hat{\Gamma}_{\alpha'}]$, to our resonance model [as defined in Eq. (11)] gives the standard Breit-Wigner²⁸ result (see, e.g., Ref. 34):

$$\mathcal{T}_{\alpha\alpha'} = -\int dE f'(E) \frac{\Gamma_{\alpha'} \Gamma_\alpha}{(E - E_0)^2 + (\Gamma/2)^2}. \quad (18)$$

Let us consider for simplicity an example of L single-mode leads. By using the multiterminal Landauer conductance formula⁴⁰ for spinless electrons, $\mathcal{G}_{\alpha\alpha'} = (e^2/h) \mathcal{T}_{\alpha\alpha'}$, in Eq. (18), we recover well-established³⁴ results for the peak conductance of a strongly pinched QD, that are related to Eq. (16) in an extremely simple way:

$$\mathcal{G}_{\alpha\alpha'}^{\text{peak}} = \frac{e^2}{h} \frac{4\Gamma_\alpha \Gamma_{\alpha'}}{\Gamma D} \equiv \frac{4\Gamma}{hD} \Delta Q_\alpha^{\text{res}} \Delta Q_{\alpha'}^{\text{res}}, \quad (19)$$

where

$$D = \begin{cases} \Gamma, & kT \ll \Gamma, \\ (8/\pi)kT, & kT \gg \Gamma. \end{cases} \quad (20)$$

Measurements of the peak conductance at a particular resonance point for fixed temperature and all possible combinations of source and drain leads would give, in principle, $(L^2 - L)/2$ experimental values to be used in Eqs. (19). Together with Eq. (17), this gives $(L^2 - L)/2 + 1$ equations for the $L + 1$ unknowns $\Delta Q_\alpha^{\text{res}}$ and Γ/D . Measurement of the temperature dependence of $\mathcal{G}_{\alpha\alpha'}^{\text{peak}}(T)$ would yield $D(T)$, and thus determine Γ . We see that even for $L = 2$ it is possible to predict the adiabatically pumped charge from the conductance measurements, and for $L > 2$ different cross checks become feasible.

Additional input of a few bits of information is necessary to make the solution of Eqs. (19) and (17) unique. For a specific resonance “res,” all the charges $\Delta Q_\alpha^{\text{res}}$ (for all α) have the same sign, determined by the type of the resonance: “+” for loading and “-” for unloading, see Eq. (16). An additional sign uncertainty arises in the case of two terminals ($\alpha = l, r$): the respective equation for the pumped charge, $\Delta Q_l(e - \Delta Q_r) = \mathcal{G}_{lr}^{\text{peak}}(hD/4\Gamma)$, is symmetric under inversion, $l \leftrightarrow r$. The resolution of these uncertainties depends on the particular experimental situation, and should be easy in simple cases. We illustrate this point in Sec. (IV) below, when we discuss a two-terminal example.

C. Adiabaticity condition

One condition for the validity of the adiabatic picture requires that an electron should have enough time to tunnel under the barriers while the system is at resonance. Thus, the inverse tunneling rate \hbar/Γ should be much smaller than the duration of the resonance, $\tau_r = D/|\dot{E}_0|$, yielding the adiabaticity condition,

$$\hbar|\dot{E}_0| \ll \Gamma D. \quad (21)$$

This condition implies that both the amplitude and the frequency of the pumping potential must be sufficiently small for an adiabatic pump.²⁶ The resonance duration τ_r can be extracted from measurements of the conductance as follows: measuring the variation of the conductance through the resonance, using a very low frequency ω_0 , would yield the resonance width τ_{r0} for that frequency. The value of τ_r relevant for the pumping experiments can then be found by rescaling, $\tau_r = \tau_{r0}\omega_0/\omega$.

At zero temperature, $D = \Gamma$ and the condition (21) can be compared to the adiabaticity criterion for coherent pumping formulated recently by Moskalets and Büttiker.³¹ They consider the number of sidebands n_{max} required to describe adequately the Fourier transform of the instantaneous scattering matrix. In our case the resonant peak of transmission in the time domain has the width τ_r , and the number of relevant Fourier harmonics n_{max} is at least $(\omega\tau_r)^{-1}$, where ω is the cyclic frequency of the pump. The adiabaticity criterion of Ref. 31 states that the scattering matrix should vary little with energy over the range $E \pm \hbar\omega n_{\text{max}}$. Since our characteristic energy scale for the scattering matrix is Γ , the condition of Ref. 31 takes the form $\Gamma \gg \hbar\omega n_{\text{max}} = \hbar\tau_r^{-1}$, equivalent to Eq. (21).

D. Application to complicated pumping potentials

In the resonance approximation, the pumped charge is expressed in terms of the resonance *points*, where the pumping contour crosses the resonance lines, and do not require the full information on the contour in the parameter space. We now discuss the conditions under which Eq. (16) can be used to obtain efficient approximate estimates of the pumped charge for a model Hamiltonian \mathcal{H}^d , which is complicated enough to render an exact integration²⁵ of Eq. (6) impractical. Even when the validity of the resonance approximation is marginal, such an approximate estimate could provide a handy tool for exploring complicated pumping models (e.g., Refs. 11,16 and 25) and identifying the relevant physical parameters. For simplicity, we restrict this discussion to zero temperature.

To leading order in the coupling strengths λ_α , the parameters of the resonant level in Eq. (11) are given by the eigenstate of the decoupled $\mathcal{H}^d(t)$ which is the closest to the Fermi energy μ . Therefore, the following algorithm can be formulated.

- (1) Diagonalize $\mathcal{H}^d(t)$ (analytically or numerically) to get the spectrum $\{\epsilon_m(t), |\psi_m(t)\rangle\}$.
- (2) Calculate the time-dependent decay widths $\Gamma_\alpha^m(t) = \langle \psi_m(t) | \hat{\Gamma}_\alpha(E = \mu) | \psi_m(t) \rangle$ and shifted energy levels $\epsilon'_m(t) = \epsilon_m(t) + \langle \psi_m(t) | \hat{\mathcal{E}}(E = \mu) | \psi_m(t) \rangle$.
- (3) For every m , find all such times $t_{m,j}$ when the resonance condition $\epsilon'_m(t_{m,j}) = \mu$ is satisfied.
- (4) At each resonance time $t = t_{m,j}$, compute the corresponding partial charge $q_{\alpha}^{m,j} = e\Gamma_\alpha^m / \sum_{\alpha'} \Gamma_{\alpha'}^m$.
- (5) Calculate the total pumped charge as

$$Q_\alpha^R = - \sum_{m,j} q_{\alpha}^{m,j} \text{sgn } \dot{\epsilon}'_m(t_{m,j}), \quad (22)$$

or set $Q_\alpha^R = 0$ if no resonances were found in step 3.

The application of this algorithm is justified under the conditions listed in the beginning of this section. The most important condition is the consistency of the perturbation expansion, $\Gamma_\alpha^m(t_{m,j}) \ll \Delta(t_{m,j})$, where $\Delta(t)$ is the level spacing of $\mathcal{H}^d(t)$ at the Fermi surface.

The algorithm will fail for certain values of the adjustable (not pumping) parameters of the model, for which the number of resonance points found in step 3 changes. This change corresponds to the appearance (or annihilation) of a pair of loading/unloading resonances. Such a crossover is usually manifested by a sharp change (a step) (Refs. 16,25) in the total pumped charge, as function of the model parameters.

IV. EXAMPLE: TURNSTILE MODEL

We illustrate the resonance approximation by a simple example of a single energy level with adiabatically varying couplings to the left and right reservoirs (single level turnstile model).¹⁵ Applications to more complicated models, such as pumping by surface acoustic waves,²⁵ will be reported elsewhere.

A. The turnstile pumping model

The single level turnstile model, discussed in Ref. 15, can be described as a special case of the general Hamiltonian (1), with $N=1$ site (and a single energy $h_{11}=\epsilon$) on the QD and with $L=2$ leads, denoted by $\alpha=l,r$. It is now convenient to use a slightly different notation: Consider an infinite chain of TB sites, enumerated by $n=0,\pm 1,\dots$. The site $n=0$, which represents the QD, has a time-independent energy ϵ and defines $\mathcal{H}_{\text{res}}^d = \epsilon d^\dagger d$, with eigenstate $|\psi\rangle$. The sites with $n>0$ ($n<0$) form the right (left) single-mode TB lead:

$$\mathcal{H}_\alpha^l = - \sum_{n=\pm 1}^{\pm \infty} J(c_n^\dagger c_{n\pm 1} + c_{n\pm 1}^\dagger c_n), \quad (23)$$

where the upper sign refers to $\alpha=r$. The coupling operators are $L_\alpha = \sqrt{X_\alpha(t)} J c_{\pm 1}^\dagger d$, with the two time-dependent pumping parameters $X_\alpha = \lambda_\alpha^2$.

The Hamiltonian of the leads (23) is characterized by the dispersion relation $E_k = -2J \cos ka$ and the retarded Green function

$$[G_\alpha^l]_{nm} = \frac{e^{ika|n-m|} - e^{-ika|m+n|}}{i2J \sin ka}, \quad (24)$$

where a is the nearest-neighbor distance. The self-energy operator [Eq. (8)] is $\hat{\Sigma} = -(X_l + X_r) J e^{ika} d^\dagger d$.

We consider the zero-temperature limit and parametrize the on-site energy as $\epsilon = (-2 + \delta) J \cos \kappa a$, where the dimensionless parameter δ is a measure of the detuning of the isolated level ϵ from the Fermi energy $\mu = -2J \cos \kappa a$ in the leads. Near the band bottom one has $\delta \approx (\epsilon - \mu)/J$.

The resonance parameters at the Fermi surface are

$$\Gamma_\alpha = 2X_\alpha J \sin \kappa a,$$

$$E_0 = (-2 + \delta - X_l - X_r) J \cos \kappa a. \quad (25)$$

Both Γ_α and E_0 depend on time via the time-dependent couplings X_α , which span the parameter space $\{X_l, X_r\}$. The resonance condition $E_0 = \mu$ defines the resonance line, $X_l + X_r = \delta$. For an explicit calculation, we next choose the pumping contour to be a square with corners at points $A(X_1; X_1)$ and $C(X_2; X_2)$, as used in Ref. 15. [This is shown in Fig. 2(a), which forms an explicit example of Fig. 1].

The necessary conditions of Sec. III, for having distinct resonances, are satisfied only at the bottom of the TB band ($\sin \kappa a \ll \cos \kappa a$). As we gradually increase δ from zero, the resonance line in Fig. 2(a) moves in the direction indicated by the small arrow. The resonance line crosses the contour only if $2X_1 \equiv \delta_1 < \delta < \delta_3 \equiv 2X_2$. Therefore, within the resonance approximation we have

$$Q^R/e = 0, \text{ if } \delta < \delta_1 \text{ or } \delta > \delta_3. \quad (26)$$

For the direction of the contour shown by the arrows in Fig. 2(a), the resonance point B corresponds to loading of the dot mostly from the left ($\Gamma_l > \Gamma_r$). Its complementary resonance point D is associated with unloading mostly to the right ($\Gamma_l < \Gamma_r$). This interpretation is illustrated in Fig. 2(b).

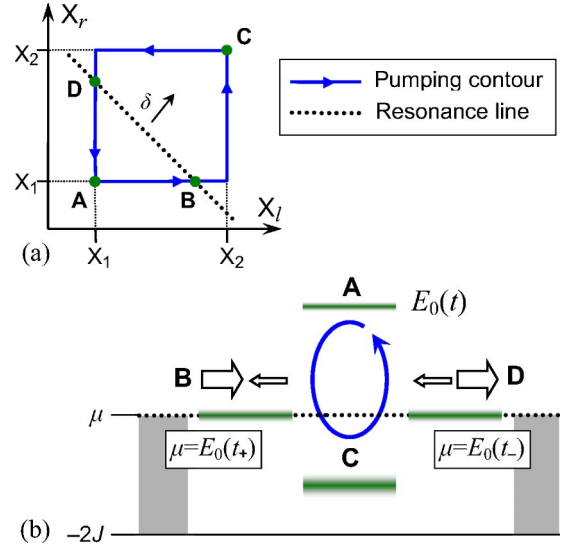


FIG. 2. (Color online) (a) The pumping contour A - B - C - D - A and the resonance line B - D for the single level turnstile model (Ref. 15). (b) Interpretation of the pumping cycle on an energy diagram. (a) The effective energy level E_0 is above the chemical potential μ , the dot is empty. (b) Loading process with preference to the left-coming electrons. (c) The level E_0 is below μ , the dot is occupied. (d) Unloading process with preference to the right-going electrons. The asymmetry between B and D creates the nonvanishing total pumped charge. The arrows indicate schematically the direction and the relative magnitude of the current pulses caused by each resonance.

At the lower left part of the contour, $\delta < \delta_2 = (\delta_1 + \delta_3)/2 = X_1 + X_2$, the resonance points are $D(X_1, \delta - X_1)$ and $B(\delta - X_1, X_1)$. The partial charges pumped from the left [using Eqs. (16) and (25)] are

$$\Delta Q_l^D = -e \frac{2X_l J \sin \kappa a}{2(X_l + X_r) J \sin \kappa a} = -e \frac{X_l}{\delta}, \quad (27)$$

$$\Delta Q_l^B = e \frac{\delta - X_1}{\delta}, \quad (28)$$

where we have used $\text{sgn} \dot{E}_0 = \text{sgn}(d/dt)(-X_l - X_r) = +1$ for point D . The net pumped charge is thus

$$Q^R/e = Q_l^R/e = (\Delta Q_l^D + \Delta Q_l^B)/e = -Q_r^R/e = e - (\delta_1/\delta), \text{ if } \delta_1 < \delta < \delta_2. \quad (29)$$

A similar analysis for crossing at $D(\delta - X_2, X_2)$ and $B(X_2, \delta - X_2)$ (when $\delta_2 < \delta < \delta_3$) yields

$$Q^R/e = (\delta_3/\delta) - 1, \text{ if } \delta_2 < \delta < \delta_3. \quad (30)$$

Our resonance approximation results for Q^R/e are shown for some typical parameters (together with the exact results, see below) in Fig. 3. These results agree qualitatively with those of Refs. 11 and 16: Q^R/e reaches its maximum value $(X_2 - X_1)/(X_1 + X_2)$ at $\delta = \delta_2$, where the resonance points B and D are farthest away from the resonance point M , which occurs at $X_1 = X_2 = \delta/2$. Note that Q^R/e approaches the

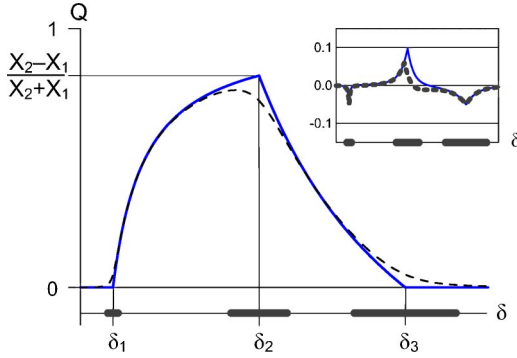


FIG. 3. (Color online) Pumped charge (in units of e) as a function of δ for $X_1=1/50$, $X_2=1/5$, and $\kappa a = \pi/20$, calculated within the resonance approximation (Q^R , blue continuous line) and exactly (Q , dashed line). Thick bars on the δ axis mark the resonance widths $\pm\Gamma/J$ around the special points $\delta_{1,2,3}$, where deviations from the exact result are anticipated. Inset: Absolute error of the resonance approximation $(Q^R - Q)/e$ for the same values of δ . The thick dotted line corresponds to Q^R calculated from the transmission maxima, see text for details.

quantized value 1 when $X_2/X_1 \rightarrow \infty$, i.e., when the transmission at the resonance points [related to $4X_1X_2/(X_1+X_2)^2$, via Eq. (18)] vanishes. This is consistent with Ref. 11, which required that “a large part of the resonance line” be surrounded by the pumping contour.

B. Comparison with exact results

The formula (13) for the resonance current is exact in our case. Substitution of Eq. (25) into Eq. (13) and integration over the contour A - B - C - D gives the total pumped charge in the form

$$Q = \frac{e}{\pi} \int dX [F(X, X_1) - F(X, X_2)], \quad (31)$$

where

$$F(X, Z) = \frac{(\delta - 2Z) \sin \kappa a \cos \kappa a}{(\delta - X - Z)^2 \cos^2 \kappa a + (X + Z)^2 \sin^2 \kappa a}. \quad (32)$$

This result was obtained in Ref. 15 using the time derivatives of the scattering matrix.

In Fig. 3 we compare the exact Q and the approximate Q^R . As the resonance line in Fig. 2(a) moves from point A to C , the pumped charge rises from zero to a maximum, close to $(X_2 - X_1)/(X_2 + X_1)$, and then falls back towards zero. Except for the vicinity of the special points $\delta = \delta_1, \delta_2$, and δ_3 , there is an excellent agreement between Eqs. (26), (29), and (30), and Eq. (31).

The most significant source for deviations of the exact pumped charge Q from the separated resonance result Q^R is the term proportional to $\dot{\Gamma}_\alpha$ in the expression of the pumping current (13):

$$Q - Q^R \approx \frac{e}{2\pi} \int \frac{d\Gamma_\alpha(E_0 - \mu)}{(\mu - E_0)^2 + (\Gamma/2)^2}. \quad (33)$$

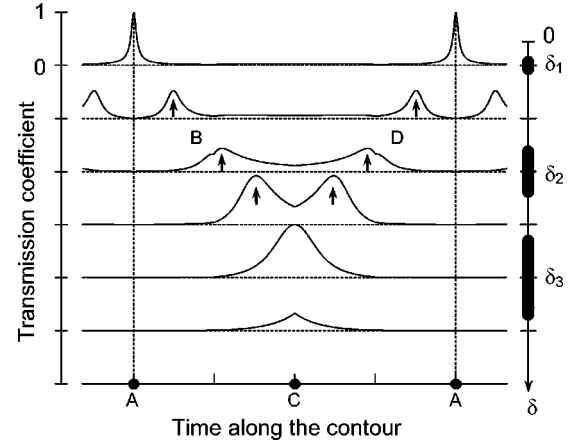


FIG. 4. Time traces of the transmission coefficient T_{tr} along the pumping contour for six values of δ , increasing with constant intervals from top to bottom. Two complementary resonances B and D (marked with arrows) are observed for $\delta_1 < \delta < \delta_3$ when the pumping contour crosses the resonance line [cf. Fig. 2(a)]. Thick bars on the δ axis mark the regions where the loading/unloading pumping mechanism fails.

In our example, Eq. (25) yields $d\Gamma_\alpha/dE_0 = \dot{\Gamma}_\alpha/\dot{E}_0 = -2 \tan(\kappa a)$ when the resonance is on an edge of the contour curve where only X_α varies. Thus, the integral in Eq. (33) is negligibly small as long as the distance between the resonance point and a corner of the square contour is larger than Γ/J . Indeed, this agrees with Fig. 3, where the regions $|\delta - \delta_i| < \Gamma/J$ are indicated by horizontal bars on the δ axis.

Figure 4 shows the Breit-Wigner transmission coefficient T_{tr} , calculated from Eqs. (18) and (25) as a function of time (defined homogeneously along the pumping contour) for several values of δ . As δ is increased from zero, a single peak develops at $\delta = \delta_1$, then splits into two independent resonances B and D , which move along the pumping contour and finally merge at $\delta = \delta_3$ and disappear. By comparing Fig. 4 to Fig. 3 one can follow the correlation between the presence of separate well-defined transmission peaks and the validity of the resonance approximation for the pumped charge.

C. Relation to transmission

The quantitative relation between the pumped charge and the transmission (conductance) has been discussed in Sec. III B. In order to illustrate this discussion, let us assume that the transmission traces (Fig. 4) are the *only* available data for our two terminal system. One observes two resonances in the range $\delta_1 < \delta < \delta_3$ —both giving the same value of the peak transmission T_{\max} . One of the resonances represents loading, contributing $\Delta Q_\alpha^{\text{res}} > 0$, while the other one necessarily represents unloading (with $\Delta Q_\alpha^{\text{res}} < 0$). If we make a mistake at this stage and take the wrong sign in Eq. (17), it will only change the assumed pumping direction, $Q^R \rightarrow -Q^R$. Let us treat the first resonance as loading and calculate the partial charge pumped from the left reservoir, $\Delta Q_l^{\text{res}} > 0$. Solution of Eqs. (17) and (19) gives two roots, $\Delta Q^{\text{res}} = e(1 \pm \sqrt{1 - T_{\max}})/2$, and one must decide which of the two corresponds to ΔQ_l^{res} . The same dilemma holds for the second

resonance. Considering all four options yields three possible answers $Q^R = \pm Q'$ and 0, where $Q' = e\sqrt{1 - \mathcal{T}_{\max}}$. The correct result ($Q^R = Q'$) may be chosen as the one which gives the best fit to the data of the pumping calculation/experiment. Once the uncertain signs have been chosen correctly, there is no need to repeat this “trial-and-error” procedure, since the contour changes continuously. Of course, if some features of the pumping contour design are known (such as which coupling is dominant in different regions), the sign uncertainties are much easier to resolve.

The result of the above calculation $|Q - Q^R|/e$ is shown in the inset of Fig. 3 by a thick dotted line. One can see that both ways of calculating Q^R [from the analytic expressions (26), (29), and (30) and from using the peak transmission] give similar small deviations from the exact value Q of the pumped charge.

We now leave our specific example, and consider Eq. (33) for a general resonance. As seen in the example, the integral in Eq. (33) becomes nonzero whenever $\gamma_\alpha = \Gamma_\alpha/\dot{E}_0$ is not a time-independent constant during the whole resonance. For nonconstant γ_α , the largest deviation $|Q - Q^R|$ arises when γ_α changes sign exactly at the resonance point $E_0 = \mu$; one then finds that $|(Q - Q^R)/Q^R| < x \max|\gamma_\alpha|$, where x is a number of order unity, which depends on the details of the contour. These considerations justify condition (3) in the beginning of Sec. III.

V. CONCLUSIONS

We have considered a general model of adiabatic quantum pumping of spinless noninteracting electrons, in the coherent resonant tunneling regime. In the limit of distinct transmission resonances along the pumping contour, the pumped charge is given by a sum of individual contributions due to each resonance. During each resonance one electron either enters or leaves the system, with the probability distribution between different reservoirs given by the corresponding tunneling rates Γ_α/\hbar .

We have clarified the role of quantum coherence in the resonance-assisted pumped charge quantization by showing that quantization arises due to population of discrete resonant states with preference to a single reservoir in each resonance. A quantitative and experimentally verifiable relation between the pumped charge and the peak conductance has been proposed. The resonance approximation also provides a simple calculational algorithm for analyzing complex pumping potentials.

Our results remain valid if (1) the spacing Δ between different resonant levels is much larger than Γ_α , kT ; (2) the relative magnitude of the couplings Γ_α to different reservoirs does not change much during a resonance; (3) the condition $\hbar\dot{E}_0 \ll \max(\Gamma, kT)$ is not violated.

Systematic extension of the resonance approximation to situations when electron-electron interactions play an essential role is a topic for further future study.

ACKNOWLEDGMENTS

This project was carried out in a center of excellence supported by the Israel Science Foundation.

APPENDIX: FORMULA FOR THE PUMPED CURRENT

In this appendix, we use standard scattering theory relations^{41,27} to derive Eq. (6) from Eq. (5). The scattering states $|\chi_{k\alpha}\rangle$ can be obtained from the Lippman-Schwinger equation

$$|\chi_{k\alpha}\rangle = (1 + GL_\alpha^\dagger)|w_{k\alpha}\rangle, \quad (\text{A1})$$

where $G = (E + i0 - \mathcal{H})^{-1}$ is the retarded Green function taken at energy $E = E_{k\alpha}$. The time t enters Eq. (A1) as a parameter.

Defining projection operators \hat{P}^d and \hat{P}_α onto the QD and onto lead α , one has

$$\begin{aligned} \mathcal{H}^d &= \hat{P}^d \mathcal{H}^d \hat{P}^d, \quad G_d = \hat{P}^d G_d \hat{P}^d, \quad \hat{P}_\alpha \mathcal{H} \hat{P}_{\alpha'} = \delta_{\alpha\alpha'} \mathcal{H}_\alpha^l, \\ L_\alpha &= L_\alpha \hat{P}^d = \hat{P}_\alpha \mathcal{H} \hat{P}^d, \quad \hat{P}^d |w_{k\alpha}\rangle = 0, \end{aligned} \quad (\text{A2})$$

and therefore

$$M_\alpha^d \equiv \langle \chi_{k\alpha} | \mathcal{H}^d | \chi_{k\alpha} \rangle = \langle w_{k\alpha} | L_\alpha G_d^\dagger \mathcal{H}^d G_d L_\alpha^\dagger | w_{k\alpha} \rangle. \quad (\text{A3})$$

To derive Eq. (7), we start from $(E - \mathcal{H})G = I$, multiply from the right by \hat{P}^d and from the left by \hat{P}_α and—using the identity $\hat{P}^d + \sum \hat{P}_\alpha = I$ —obtain the relation $\hat{P}_\alpha G \hat{P}^d = G_\alpha^l L_\alpha G_d$. A similar multiplication from the left by \hat{P}^d then yields Eq. (7), with

$$\hat{\Sigma} = \sum_\alpha L_\alpha^\dagger G_\alpha^l L_\alpha, \quad (\text{A4})$$

which is equivalent to Eq. (8).

Similarly, the time dependance of the coupling strengths $\lambda_\alpha(t)$ contributes to the current I_α via the matrix element $M_\alpha^l = \sum_{\alpha'} \langle \chi_{k\alpha} | \dot{L}_{\alpha'} | \chi_{k\alpha} \rangle + \text{H.c.}$ Using the trivial relations $\dot{L}_\alpha = (\dot{\lambda}_\alpha/\lambda_\alpha)L_\alpha$ and $\hat{P}_{\alpha'} |w_{k\alpha}\rangle = \delta_{\alpha\alpha'} |w_{k\alpha}\rangle$, a straightforward calculation gives

$$M_\alpha^l = \langle w_{k\alpha} | L_\alpha \left[G_d^\dagger \dot{\mathcal{E}} G_d L_\alpha^\dagger + \frac{\dot{\lambda}_\alpha}{\lambda_\alpha} (G_d + G_d^\dagger) \right] L_\alpha^\dagger | w_{k\alpha} \rangle. \quad (\text{A5})$$

The normalization to the unit flux $\langle w_{k\alpha} | w_{k'\alpha} \rangle = (2\pi/v_{k\alpha})\delta(k - k')$ implies that $\hat{P}_\alpha = \int (dk/2\pi) v_{k\alpha} |w_{k\alpha}\rangle \langle w_{k\alpha}|$. Using also the standard relation $i(G_\alpha^l - G_\alpha^{l\dagger}) = |w_{k\alpha}\rangle \langle w_{k\alpha}|/\hbar$, we find the relation

$$\hbar \hat{\Gamma}_\alpha = L_\alpha^\dagger |w_{k\alpha}\rangle \langle w_{k\alpha}| L_\alpha. \quad (\text{A6})$$

Introducing the trace over the QD's subspace, using Eq. (A6) in Eqs. (A3) and (A5), and substituting the results into $\mathcal{I}_\alpha = (M_\alpha^d + M_\alpha^l)/\hbar$, we finally end up with Eq. (6).

- ¹M. Switkes, C.M. Marcus, K. Campman, and A.C. Gossard, *Science* **283**, 1905 (1999).
- ²L.P. Kouwenhoven, A.T. Johnson, N.C. van der Vaart, C.J.P.M. Harmans, and C.T. Foxon, *Phys. Rev. Lett.* **67**, 1626 (1991).
- ³R.L. Kautz, M.W. Keller, and J.M. Martinis, *Phys. Rev. B* **60**, 8199 (1999), and references therein.
- ⁴I.L. Aleiner and A.V. Andreev, *Phys. Rev. Lett.* **81**, 1286 (1998).
- ⁵P.W. Brouwer, *Phys. Rev. B* **58**, 10 135 (1998).
- ⁶F. Zhou, B. Spivak, and B. Altshuler, *Phys. Rev. Lett.* **82**, 608 (1999).
- ⁷B.L. Altshuler and L.I. Glazman, *Science* **283**, 1864 (1999).
- ⁸T.A. Shutenko, I.L. Aleiner, and B.L. Altshuler, *Phys. Rev. B* **61**, 10 366 (2000).
- ⁹Y. Wei, J. Wang, and H. Guo, *Phys. Rev. B* **62**, 9947 (2000).
- ¹⁰M. Moskalets and M. Büttiker, *Phys. Rev. B* **64**, 201305 (2001).
- ¹¹Y. Levinson, O. Entin-Wohlman, and P. Wölfe, *Physica A* **302**, 335 (2001).
- ¹²J.E. Avron, A. Elgart, G.M. Graf, and L. Sadun, *Phys. Rev. Lett.* **87**, 236601 (2001).
- ¹³Y. Makhlin and A.D. Mirlin, *Phys. Rev. Lett.* **87**, 276803 (2001).
- ¹⁴B. Wang, J. Wang, and H. Guo, *Phys. Rev. B* **65**, 073306 (2002).
- ¹⁵O. Entin-Wohlman, A. Aharony, and Y. Levinson, *Phys. Rev. B* **65**, 195411 (2002).
- ¹⁶O. Entin-Wohlman and A. Aharony, *Phys. Rev. B* **66**, 035329 (2002).
- ¹⁷P. Sharma and C. Chamon, *Phys. Rev. B* **68**, 035321 (2003).
- ¹⁸M. Ya. Azbel', *Europhys. Lett.* **18**, 537 (1992).
- ¹⁹J. Wang and B. Wang, *Phys. Rev. B* **65**, 153311 (2002).
- ²⁰M. Blaauboer, *Phys. Rev. B* **65**, 235318 (2002).
- ²¹M. Blaauboer and E.J. Heller, *Phys. Rev. B* **64**, 241301 (2001).
- ²²T. Aono, *Phys. Rev. B* **67**, 155303 (2003).
- ²³A. Banerjee, S. Das, and S. Rao, *cond-mat/0307324* (unpublished).
- ²⁴D.V. Averin and K.K. Likharev, in *Mesoscopic Phenomena in Solids*, edited by B.L. Altshuler, P.A. Lee, and R.A. Webb (Elsevier, Amsterdam, 1991), p. 173.
- ²⁵A. Aharony and O. Entin-Wohlman, *Phys. Rev. B* **65**, 241401 (2002).
- ²⁶O. Entin-Wohlman, A. Aharony, and V. Kashcheyevs, *J. Phys. Soc. Jpn.* **72A**, 77 (2003).
- ²⁷S. Datta, *Electronic Transport in Mesoscopic Systems* (Cambridge University Press, Cambridge, 1997).
- ²⁸G. Breit and E. Wigner, *Phys. Rev.* **49**, 519 (1936).
- ²⁹A.D. Stone and P.A. Lee, *Phys. Rev. Lett.* **54**, 1196 (1985).
- ³⁰M. Büttiker, *IBM J. Res. Dev.* **32**, 63 (1988).
- ³¹M. Moskalets and M. Büttiker, *Phys. Rev. B* **66**, 205320 (2002).
- ³²B. Wang, J. Wang, and H. Guo, *Phys. Rev. B* **68**, 155326 (2003).
- ³³S.A. Wolf, D.D. Awschalom, R.A. Buhrman, J.M. Daughton, S. von Molnár, M.L. Roukes, A.Y. Chtchelkanova, and D.M. Treger, *Science* **294**, 1488 (2001).
- ³⁴Y. Alhassid, *Rev. Mod. Phys.* **72**, 895 (2000).
- ³⁵H.A. Weidenmüller, *Phys. Rev. B* **65**, 245322 (2002).
- ³⁶C.A. Stafford, *Phys. Rev. Lett.* **77**, 2770 (1996).
- ³⁷A.P. Klein and A.J. Heeger, *Phys. Rev.* **144**, 458 (1966).
- ³⁸B. Wang and J. Wang, *Phys. Rev. B* **65**, 233315 (2002).
- ³⁹A. Alekseev, *cond-mat/0201474* (unpublished).
- ⁴⁰M. Büttiker, *Phys. Rev. Lett.* **57**, 1761 (1986).
- ⁴¹M. Paulsson, *cond-mat/0210519* (unpublished).
- ⁴²A.-P. Jauho, N.S. Wingreen, and Y. Meir, *Phys. Rev. B* **50**, 5528 (1994).
- ⁴³B. Wang, J. Wang, and H. Guo, *J. Appl. Phys.* **86**, 5094 (1999).
- ⁴⁴M. Büttiker, H. Thomas, and A. Prêtre, *Z. Phys. B: Condens. Matter* **94**, 133 (1994).
- ⁴⁵Distinct charge steps during the pumping cycle have been presented in Ref. 25, but with no detailed quantitative discussion of their relation to resonances.
- ⁴⁶Equation (6) can be used to demonstrate the equivalence between the formalism used in Refs. 15, 25, 16 and 26 and the adiabatic limit of the Keldysh nonequilibrium Green function techniques (Refs. 42,38). Without loss of generality one can set $\dot{\lambda}_\alpha=0$, and use the cyclic property of the trace in Eq. (6). Extending the trace to the whole system and multiplying the result by 2 to restore spin degeneracy gives the charge injected into the system during an infinitesimal time δt as $\delta Q_\alpha = -(e/\pi)\int dE f'(E)\text{Tr}[G^\dagger \hat{\Gamma}_\alpha G \hat{H} \delta t]$. This is identical to Eq. (4) of Ref. 38, which in turn was proved (Refs. 38,43) equivalent to the Brouwer formulas (Refs. 5,44).
- ⁴⁷The use of the equilibrium ρ is justified because adiabatic pumping is invariant to the rescaling of time and can always be performed quasistatically.